DESIGN, SYNTHESIS, MOLECULAR DOCKING AND ANTI-PROLIFERATIVE EVALUATION OF NOVEL PYRAZOLO[4,3-E][1,2,4]TRIAZOLO[4,3-C]PYRIMIDINE DERIVATIVES AS POTENTIAL DNA INTERCALATORS AND TOPOISOMERASE II INHIBITORS

Ashraf H. Bayoumi, *Farag F. Sherbiny, Eslam B. Elkaeed, Ahmed A. Gaber

Department of Organic Chemistry, Faculty of Pharmacy (Boys), Al-Azhar University, Cairo, Egypt.

***Corresponding author**: **Dr-farag-sherbiny@azhar.edu.eg**

ABSTRACT

A series of novel hybrid pyrazolotriazolopyramidine derivatives was designed and synthesized in synthetically useful yields. All the new synthesized compounds were biologically evaluated *in vitro* for their cytotoxic activities against a panel of three cancer cell lines namely, HepG-2, MCF-7, and HCT-116. The results of cytotoxic evaluation indicated that compounds **12**, and **11** exhibited the most prominent cytotoxic effect against all tested cell lines with IC_{50} values ranging from 12.41 to 22.18 µM comparable to that of doxorubicin as a control drug (IC_{50} values of 8.17 and 9.27 µM). Moreover, the most potent compound was further evaluated for its topoisomerase II inhibitory activities and DNA intercalating affinities as potential mechanisms for its anti-proliferative activities. In particular, compound **12** exhibited higher intercalative activity with IC_{50} value of 30 µM than doxorubicin (31 µM). Interestingly, compound **12** displayed a significant topoisomerase II inhibitory activity with IC_{50} value of 0.055 µM. Furthermore, molecular docking study was also performed in order to understand the binding mode in the active site and explain the anti-cancer results with prospective target.

Keywords: Anticancer, Pyrazolotriazolopyramidine derivatives, Topoisomerase II, DNA-intercalator, Molecular docking

GRAPHICAL ABSTRACT

Compound **12** possesses the highest cytotoxic potency against all tested cell lines with IC_{50} values of 12.41, 14.23, and 15.18 µM respectively, which was additionally estimated for its DNA intercalating affinities with IC_{50} value of 30.8 µM and for topoisomerase II inhibitory activities with IC_{50} value of 0.055 µM.

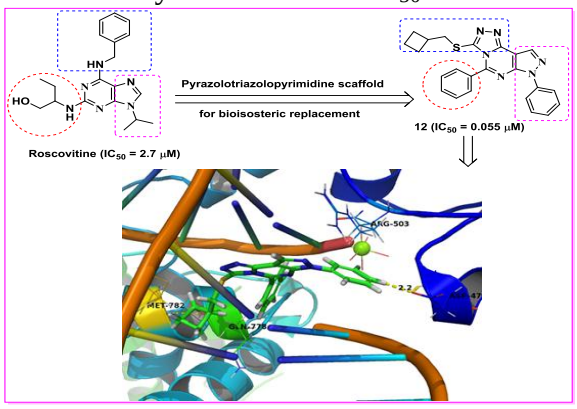

INTRODUCTION

Cancer remains one of the most common causes of death throughout the world and thus the development of potent and more effective anticancer agents represents one of the most important challenges in therapeutics due to the unrivaled pathophysiology of tumors and the predictable emergence of resistance to medication (Thun et al. 2010). Classical methods for cancer treatment including radiotherapy, chemotherapy, and immunotherapy with their own limitations.

Anticancer drugs have been classified into two main target types: the first one is drugs that target DNA, RNA, or proteins. The second target includes other elements involved in the carcinogenesis process, such as the immune system, the endothelium and the extracellular matrix. Most classical chemotherapeutic agents interact with tumour DNA (Espinosa et al. 2003). Compounds that affect DNA include groove binders, alkylating agents, DNA intercalators, and topoisomerase inhibitors (Hurley 2002).

Topoisomerases are important nuclear enzymes, which play a pivotal role in DNA replication, transcription, chromosome segregation, and recombination. There are two fundamental types of topoisomerases; (a) topoisomerase I (Topo I), which is responsible for cleavage, relaxing, and releasing of one strand of the DNA duplex, (b) topoisomerase II (Topo II), which cleaves both strands of the DNA helix simultaneously to remove DNA supercoiling (Wang 2002). These enzymes covalently bind to DNA helix via tyrosine residues in the active site. These linkages are transient and easily reversible, and the covalently bound structure is known as the cleavable complex (Denny 2004). Accordingly, topoisomerases are considered as crucial targets for cancer chemotherapy treatments (Pommier et al. 2010). Topoisomerase inhibitors block the ligation step of the cell-cycle, generating single and double stranded breaks that harm the integrity of the genome (Mlcochova et al. 2018). Introduction of these breaks subsequently leads to apoptosis (Kaina 2003).

Some anticancer drugs targeting Topo II inhibit the enzymatic activity as a primary mode of action and are known as catalytic Topo II inhibitors (Nitiss 2009). Another type of Topo II-targeting drugs, including intercalating drugs, interfere with the enzyme's cleavage and rejoining activities by trapping the cleavable complex and thereby increasing the time of the transient Topo II-catalyzed DNA breaks. These drugs are referred to as Topo II poisons because they convert the Topo II enzyme into a DNA-damaging agent (Pommier et al. 2010, Nitiss 2009).

These class of drugs act either by topo poisoning via inter-chelation with DNA as doxorubicin (Liu et al. 1989), amsacrine (Sung et al. 2005) and mitoxantrone (Shenkenberg et al. 1986). On the other hand, drugs act as catalytic inhibitors of Top-II as TSC24 (Huang et al. 2010), HY-1 (zhao et al. 2011) and compound **I** (Islam et al. 2017)

DNA Intercalators and Topo II poisons share three common essential structural features. The first one is a planar polyaromatic system (chromophore) which is sandwiched between DNA base-pairs (Laponogov et al. 2013). The second feature is a cationic species, interacting with the negatively charged phosphate group of DNAs. The cationic center may be an amino or nitrogen containing heterocyclic group, which can be protonated at physiological pH (Lee et al. 2017). The third feature is a flexible side chain that anchors DNA (Bailly et al. 2012) (Figure 1).

On the other hand, pyrazolopyramidine moieties have anticancer activities (Schenone et al. 2014). In addition, the discovery of new therapeutic DNA intercalators

for the treatment of cancer are considered one of the most important goals in the field of medicinal chemistry (Varrica et al. 2018). Pyrazolopyramidine analogs exhibited excellent anticancer activities through DNA intercalation. Pogorelčnik and co-workers optimized the first anti-topoisomerase II pharmacophore belonging to pyrazolo[3,4-d[pyrimidine scaffold performing systematic screening to predict the bioactivity between molecule and drug target. Compound **II** was a result of this high-throughput screening (HTS) and efficacious candidate in the series of pyrazolo[3,4-d]pyrimidine which showing promising anticancer activities in hepatocellular carcinoma (HepG2) and breast cancer (MCF-7) cell lines with mean IC_{50} value of 1.30 μM. besides, its topoisomerase inhibition (Pogorelčnik et al. 2015) (Figure 2).

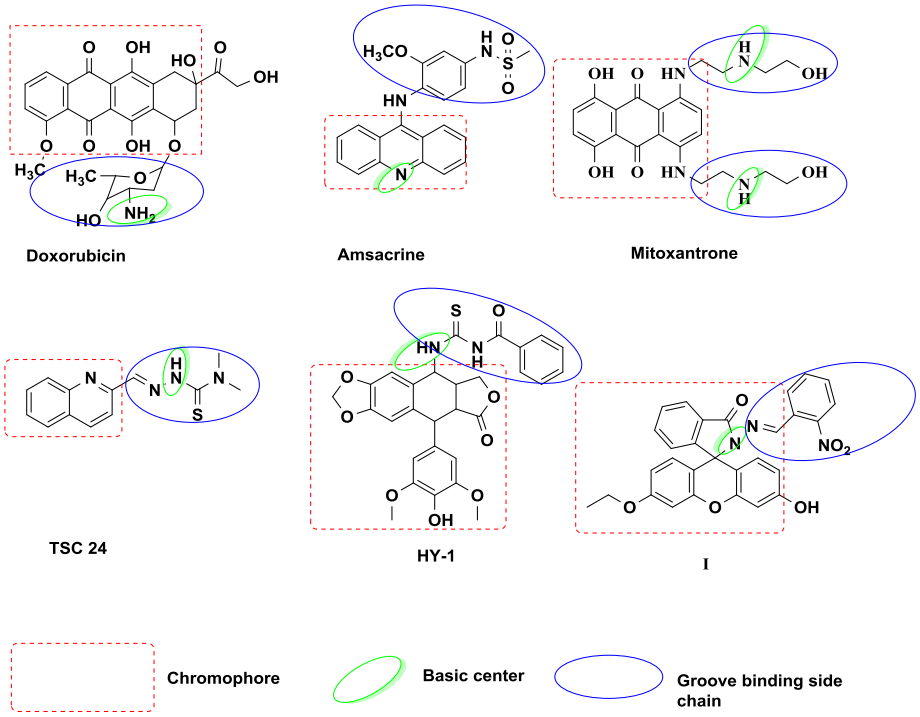

(Figure 1). DNA intercalators and their basic pharmacophoric features

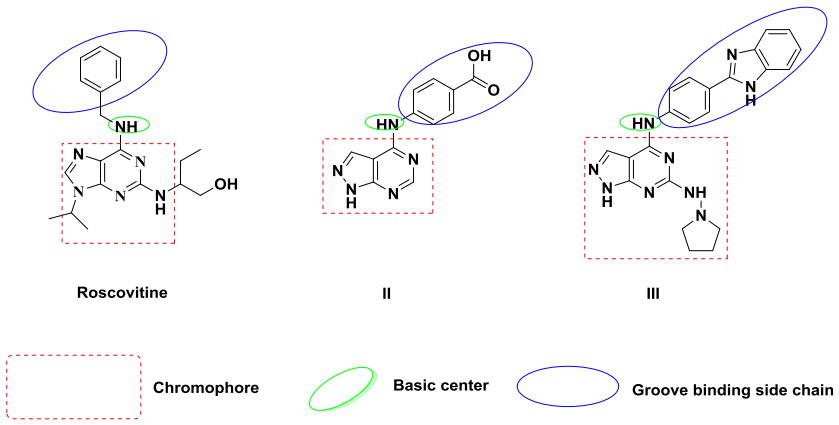

(Figure 2). Pyrimidine derivatives as topoisomerase II Inhibitors

A series of new pyrazolo[3,4-*d*]pyrimidine possessing 4-(1*H*-benzimidazol-2-yl)- phenylamine moiety at C4 position and primary as well as secondary amines at C6 position has been designed and synthesized. Their antitumor activities were evaluated against a panel of 60 human cancer cell lines. Compound **III** proved to be the most active and efficacious candidate in this series, with mean IC_{50} values of 1.30. μM Further biological evaluation suggested that this compound induce apoptosis and inhibit human topoisomerase (Topo) IIα (Singla et al. 2017). On the other hand, roscovitine, belongs to the family of purine and is used for the treatment of lung cancer with IC_{50} value of 2.7 μM (Whittaker et al. 2004).

Therefore, on the basis of previously above-mentioned findings and in resumption of our previous efforts in the design and synthesis of new anticancer agents (Gaber et al. 2018), we report the design, synthesis, DNA intercalating, and docking studies of a new series of pyrazolotriazolopyramidine derivatives. These derivatives were designed based on the main pharmacophoric features of DNA intercalators.

Rationale drug design

As reported previously, the basic influential chemical features of anti-topo II activity are indispensable for anticancer activity. Also, it is well known that triazole moiety is one of the most important chemical features necessary for anticancer activity and thus, anti-topo II activity (Huang et al. 2013) that also its effect is enhanced when fused with other heterocyclic moieties such as quinoxaline nucleus (Ibrahim et al. 2018). Therefore, the essential core of the rationale is to hybridize bioisostere pyrazolo[4,3-c[pyrimidine nucleus with the triazole moiety which display significantly different hydrogen bonding potentials in order to get an efficacious anti-topo II activity. Furthermore, some alkyl moieties, which play as groove-binding side chain, have been hybridized with pyrazolotriazolopyramidine nucleus (Figure 3).

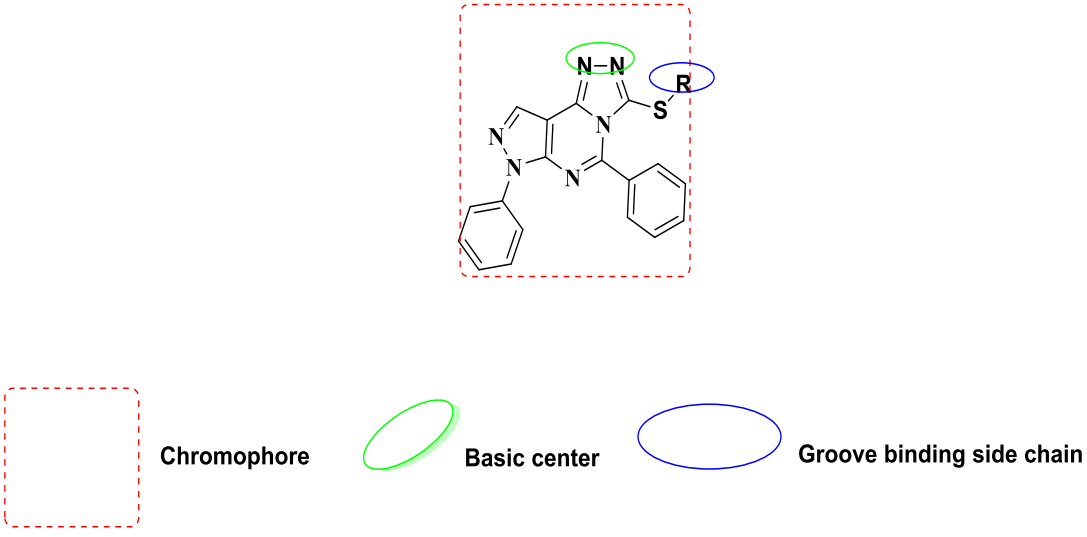

(Figure 3). Proposed rationale drug design of new potential DNA intercalators

Results and discussion

Chemistry

The designed compounds were synthesized as outlined in schemes (1, 2). Ethoxymethylene malononitrile, **1** (Ding et al. 2012) was allowed to refluxed with commercially available phenylhydrazine in ethanol to produce 5-amino-1-phenyl-1H-pyrazole-4-carbonitrile **2** (Cheng et al. 1956). Compound **2** was underwent a partial hydrolysis using alcoholic NaOH to produce carboxamide derivative **3** (He et al. 2011). 1,6-Diphenyl pyrazolo[3,4-d]pyrimidine core **4** (Miyashita et al. 1990) was formed from the reaction of compound **3** with methyl benzoate with subsequent chlorination using phosphoryl trichloride to afford compound **5** (Miyashita et al. 1998). The obtained compound **5** was heated with hydrazine hydrate to afford 4-hydrazinyl-1,6-diphenyl-1H-pyrazolo[3,4-d]pyrimidine **6** (Gaber et al. 2018). Cyclocondensation reaction of the hydrazine derivative **6** using potassium hydroxide and carbon disulphide in absolute ethanol followed by treatment with hydrochloric acid which resulted in the key intermediate compound, pyrazolo[4,3-e][1,2,4]triazolo[4,3-c]pyramidine-3-thiol **7** (scheme 1). There is tautomerism between (SH) and neighboring N of triazole moiety, so that the ^{1}H-NMR spectrum of compound **7** revealed singlet signal at 14.42 ppm (D_2O exchangeable) corresponding to thiole proton and singlet signal at 13.85 ppm (D_2O exchangeable) corresponding to (NH) proton.

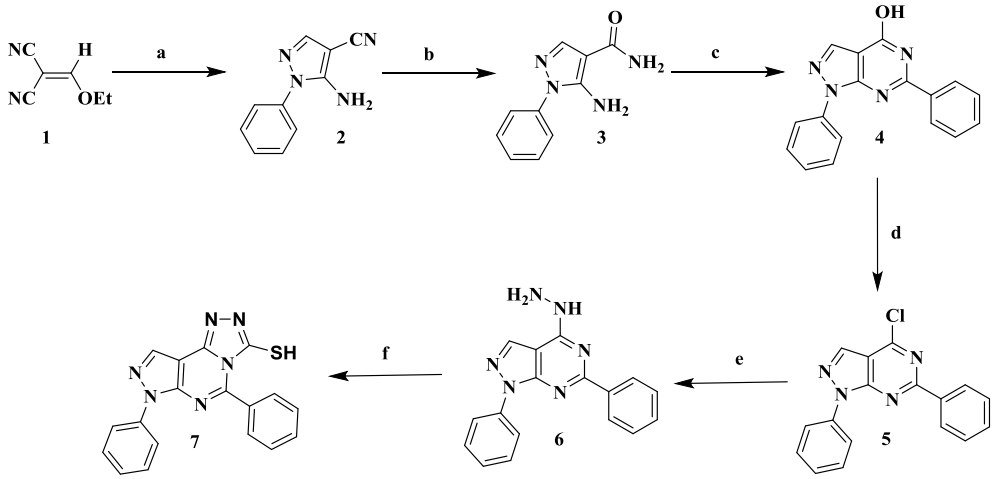

(Scheme 1). General procedure for synthesis of the key intermediate triazole derivative (**1-7**). Reagents and conditions of reaction; (a) phenyl hydrazine, absolute ethanol, reflux, 2 h; (b) sodium hydroxide, absolute ethanol, HCl, reflux, 5 h; (c) methyl benzoate, sodium ethoxide, absolute ethanol, HCl, reflux, 14 h; (d) phosphoryl trichloride, reflux, 6 h; (e) hydrazine hydrate 99%, reflux, 8 h; (f) carbon disulphide, absolute ethanol, potassium hydroxide, reflux, 16 h, hydrochloric acid

Furthermore, compounds **8-12** were prepared by the reaction of different appropriate alkyl bromides, namely, 1-bromobutane, 1-bromo-2-methylpropane, 1-bromo-2,2-dimethylpropane, bromocyclopentane and (bromomethyl)cyclobutane with compound **7** in the presence of anhydrous potassium carbonate in DMF. This reaction proceeded smoothly and the desired compounds were obtained in good yields (~ 70%) (scheme 2).

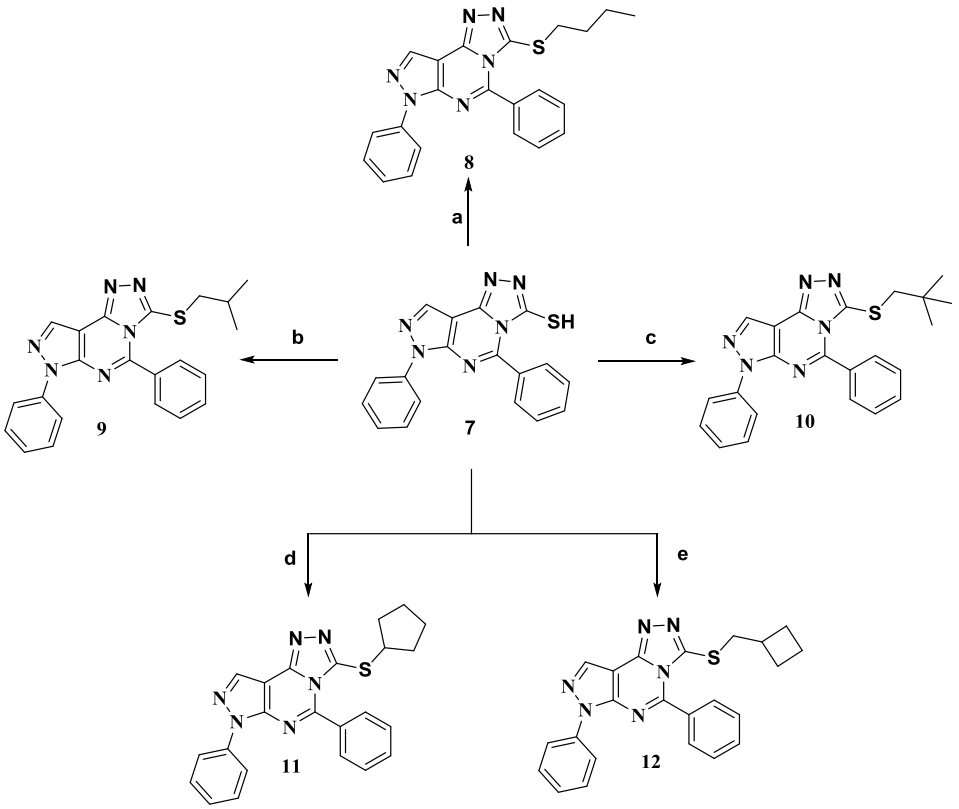

(Scheme 2). General procedure for synthesis of target compounds (**8-12**). Reaction of the triazole derivative **7** with different alkyl halides. Reagents and conditions of reaction; (a) 1-Bromobutane, (b) 1-Bromo-2-methylpropane, (c) 1-Bromo-2,2-dimethylpropane, (d) Bromocyclopentane, and (e) (Bromomethyl)cyclobutane in the presence of anhydrous potassium carbonate and DMF.

The structures of all newly synthesized compounds, (**8-12**) were confirmed by IR, ^{1}H-NMR, ^{13}C-NMR and mass spectra. For example, IR spectrum of compound **10** showed that the presence of new peak 2955 cm^{-1} specific for aliphatic -CH stretching. ^{1}H-NMR spectrum of compound **10** revealed that singlet peak at 3.41 ppm corresponding to (S-CH_2) protons and sharp singlet peak at 1.05 ppm specific for nine protons of neopentyl group and disappear of signals corresponding to thiole proton at 14.42 ppm.

Biological evaluation

In vitro antiproliferative activities

The new synthesized compounds have been *in vitro* evaluated for their anti-cancer activities against three different cancer cell lines namely, hepatocellular carcinoma (HepG-2), human breast adenocarcinoma (MCF-7) and human colon cancer (HCT-116) cells using neutral red assay Borenfreund et al. 1985). The screened compounds displayed different levels of cytotoxicity ranging from excellent, and weak activities against all tested cell lines.

Data represented in (Table 1) revealed that, compounds **11**, and **12** exhibit the highest significant cytotoxic effect against all tested cell lines with IC_{50} values ranging from 12.41 to 22.18 µM compared with doxorubicin as control drug. Compound **12** was the most potent one with IC_{50} values of 12.41, 14.23, and 15.18 µM, respectively compared with other active compounds which can be explained by important chemical

features of cyclobutylmethyl moiety which was used as a linker and required to hold binding site. As a result, the replacement of the cyclobutylmethyl moiety with other bioisostere (cyclopentyl) as compound **11** lead to almost the same potency (IC_{50} values of 18.38, 22.18, and 19.39 μM respectively). However, the substitution with butyl, isobutyl, or neopentyl moiety instead of cyclobutylmethyl moiety (**8**, **9**, **10**) might be unfavorable to cytotoxicity, indicating that the size of cyclic moiety of compound **12** was likely required for activity.

(**Table 1**) *In vitro* cytotoxicity against hepatocellular carcinoma (HepG-2), human breast adenocarcinoma (MCF-7) and human colon cancer (HCT-116) activity of new synthesized compounds.

Compound	IC_{50} (μM) HepG-2	IC_{50} (μM) MCF-7	IC_{50} (μM) HCT-116	IC_{50} (μM) DNA intercalation	IC_{50} (μM) Topo-II inhibition
7	>100	>100	>100	>100	NT_b
8	79.24±3.2	84.15±2.8	72.24±3.2	72.06±3.1	NT_b
9	61.10±2.9	70.52±2.6	65.52±2.6	53.48±2.5	NT_b
10	33.79±1.8	38.06±2.0	35.41±0.6	45.90±2.0	NT_b
11	18.38±1.0	22.18±1.3	19.38±1.0	38.62±1.7	NT_b
12	12.41±0.6	14.23±0.8	15.18±1.3	30.81±1.4	0.055±0.2
DoX	8.50±0.2	8.17±0.2	9.27±0.2	31.72±1.4	0.01±0.1

Doxorubicin (DoX) was used as positive standard. [b]Not tested

DNA intercalation activity

The synthesized compounds were tested for their DNA-binding affinities using the methyl green dye according to the reported technique (Burres et al. 1992). The DNA intercalative results displayed that the compound **12** is more intercalative than doxorubicin with IC_{50} value of 30.81 μM, whereas compounds **9**, **10** and **11** showed moderate DNA-binding activities with IC_{50} values of 53.48, 45.90, and 38.62 μM respectively. Finally, the rest of compounds were shown to possess weak DNA-binding affinities.

Topoisomerase II inhibitory activity

The most potent compound **12** was further examined as topo II inhibitors, according to the reported method (Singla et al. 2017). Doxorubicin was used as a positive control. The results of tested compound displayed that compound **12** showed good inhibitory activity with IC_{50} value of 0.055 μM compared with doxorubicin (IC_{50} = 0.01 μM).

Molecular docking

In this study, the docking of the most potent compound (**12**) with the DNA binding site of topoisomerase II (ID;3qx3), was carried out in order to predict and estimate the preferred binding mode (Ibrahim et al. 2018) . The binding site of topoisomerase II has been reported, which includes the amino acid and nucleotide residues involved in the binding interactions (Arthur et al. 2019). In particular, the compound **12** inhibits

topoisomerase by intercalating the DNA and thereby inhibiting topoisomerase in the process. The results of the docking study was reported as topoisomerase II binding free energy (ΔG).

The proposed binding mode of reference ligand, **doxorubicin**, showed affinity value equals -79.58 kcal/ mol. Doxorubicin is involved in hydrogen bonding interactions with Arg503, DA12, and DG13 and water mediated interactions with backbone amino groups of Ser480, Asp479 and Mg ion. Furthermore, **doxorubicin** made additional hydrogen bonding interactions with DT9 and DG10 and is stabilized by aromatic stacking interactions with nucleotide residues, DC8, DT9, DA12, and DG13, and hydrophobic interactions with hydrophobic part of Gln778, Met782 and Leu192 (Figure 4).

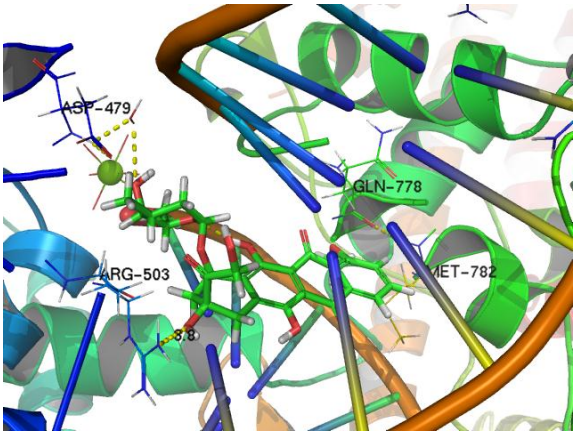

(Figure 4) Predicted binding mode of **Doxorubicin** at the binding site of topoisomerase II. H-bonds (yellow dotted lines), Hydrogen (white), nitrogen (blue), oxygen (red) and sulfur (yellow).

The suggested binding mode of compound **12** showes affinity value of -80.14 kcal/mol. It demonstrated that compound **12** is involved in a water mediated interaction DG13, and aromatic stacking interactions with nucleotide residues, DC8, DT9, DA12, and DG13. In addition, compound **12** was also stabilized by anionic π interaction with key residue, Asp479 and located in the hydrophobic pocket formed by hydrophobic parts of Arg503, and Gln778 and Met782 (Figure 5).

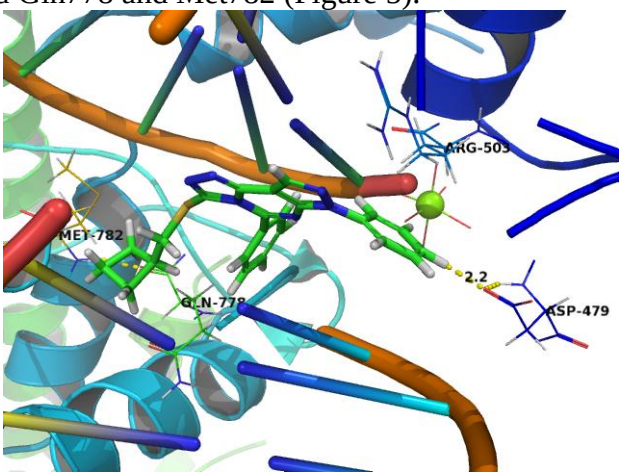

(Figure 5) Predicted binding mode of compound **12** at the binding site of topoisomerase II. H-bonds (yellow dotted lines), Hydrogen (white), nitrogen (blue), oxygen (red) and sulfur (yellow).

Experimental

Chemistry

All the chemicals which employed in this study were commercially available with analytical grade and used without any further purification. Solvents were purified and freshly distilled before using according to the standard procedures. The progress of the reaction mixtures was monitored by thin layer chromatography (TLC). The spots on the TLC plates were visualized with a UV lamp (254 nm). Melting points were measured using Thermo Fisher Scientific. IR spectra were recorded Bruker tensor 27, FT-IR Spectrophotometer. All ^{1}H NMR and ^{13}C NMR spectra were recorded on a Bruker 400 and 100 MHz Spectrophotometer. Chemical shifts (δ) are reported in parts per million (ppm) using tetramethylsilane (TMS) as an internal standard. Ultraviolet–visible (UV–vis) absorption spectra were recorded on Perkin–Elmer spectrophotometer at the wavelength of maximum absorption (λmax) in a range of DMSO at same concentrations (1×10^{-6} M). The mass spectra were run on a Shimadzu Qp 5050 Ex Spectrometer. The microanalyses for C, H and N were performed on Perkin–Elmer elemental analyzer.

Preparation of 5,7-diphenyl-7H-pyrazolo[4,3-e][1,2,4]triazolo[4,3-c]pyrimidine-3-thiol (7)

A mixture of hydrazine derivative **6** (0.3, 0.001 mol), potassium hydroxide (0.056 g, 0.001 mol) and carbon disulfide (0.12 g, 0.002 mol) in absolute ethanol (20 mL) was heated under reflux on a steam bath until the evolution of hydrogen sulfide (16 h). The excess solvent was removed by distillation and the residue was stirred with water, and filtered. The filtrate was acidified with 10 % HCl. The separated precipitate was collected, washed with water and crystallized from butanol to produce triazole derivative **7**.

Green crystal; yield 81% (0.28 g); m.p. 230-232 °C, IR (KBr, ν cm^{-1}): 3422 (NH), 3101 (Ar-H), 1193 (C=S). ^{1}H-NMR (DMSO-*d6*, δ, ppm): 7.40 – 8.53 (m, 10H, Ar-H), 8.64 (s, 1H, Ar-H, C3–H pyrazole), 13.85 (s, 1H, NH D_2O exchangeable), 14.42 (s, 1H, SH D_2O exchangeable); ^{13}C-NMR (DMSO, 100 MHz): 104.88, 123.70, 125.21, 126.11, 126.99, 129.13, 129.79, 133.96, 135.51, 138.56, 152.86, 154.50, 158.40, 167.88. MS (m/z): 344 (M^+, 28.50%), 77(100%). Anal. Calcd. For $C_{18}H_{12}N_6S$ (344): C, 62.78; H, 3.51; N, 24.40. Found: C, 62.82; H, 3.55; N, 24.43.

General procedure for the synthesis of compounds (8-12)

A mixture of compound **7** (0.34 g, 0.001 mol), anhydrous potassium carbonate (1.38 g, 0.001 mol) and appropriate alkyl bromide (0.001mol) namely, 1-bromobutane, 1-bromo-2-methylpropane, 1-bromo-2,2-dimethylpropane, bromocyclopentane and (bromomethyl) cyclobutane in DMF (20 ml) was refluxed on a water-bath for specific time. The reaction mixture was poured onto crushed ice with continuous stirring. The

obtained solid was collected by filtration and recrystallized from ethanol to give a corresponding compound.

3-(Butylthio)-5,7-diphenyl-7H-pyrazolo[4,3-e][1,2,4]triazolo[4,3-c]pyrimidine (8)

White solid; reaction time: 0.5 h yield 63% (0.25 g); m.p. 159-161°C; IR (KBr, ν cm^{-1}): 3075 (Ar-H), 2965 (Aliph-H). ^{1}H-NMR (DMSO-*d6*, δ, ppm): 0.95 (t, J = 7.46 Hz, 3H, -SCH_2-CH_2-CH_2-C**H**$_3$), 1.44 - 1.52 (m, 2H, -SCH_2-CH_2-C**H**$_2$-CH_3), 1.81 (quin, J = 7.58 Hz, 2H, -SCH_2-C**H**$_2$-CH_2-CH_3), 3.28 - 3.31 (m, 2H, -SC**H**$_2$-CH_2-CH_2-CH_3), 7.46 – 8.47 (m, 10H, Ar-H), 8.80 (s, 1H, Ar-H, C3–H pyrazole); ^{13}C-NMR (DMSO, 100 MHz): 13.56, 22.03, 25.05, 31.69, 102.51, 122.14, 127.81, 128.80, 129.95, 130.94, 131.71, 132.46, 133.83, 138.71, 146.44, 146.91, 149.70, 166.18; MS (m/z): 400 (M^+, 18.46), 279 (100.00). Anal. Calcd. for $C_{22}H_{20}N_6S$ (400): C, 65.98; H, 5.03; N, 20.98. Found: C, 65.94; H, 5.07; N, 20.95

3-(Isobutylthio)-5,7-diphenyl-7H-pyrazolo[4,3-e][1,2,4]triazolo[4,3-c]pyrimidine (9)

White solid; reaction time: 0.5 h yield 75% (0.30 g); m.p. 145-147 °C; IR (KBr, ν, cm^{-1}): 3078 (Ar-H), 2957 (Aliph-H). ^{1}H-NMR (DMSO-*d6*, δ, ppm): 1.05 (d, J = 6.85 Hz, 6H, -SCH_2-$CH(CH_3)_2$), 2.03 - 2.14 (m, 1H, -SC**H**$_2$-$CH(CH_3)_2$), 3.19 (d, J = 6.60 Hz, 2H, -SC**H**$_2$-$CH(CH_3)_2$), 7.46 – 8.43 (m, 10H, Ar-H), 8.76 (s, 1H, Ar-H, C3–H pyrazole); ^{13}C-NMR (DMSO, 100 MHz): 22.05, 28.66, 40.57, 102.58, 122.24, 127.81, 128.80, 129.95, 130.94, 131.72, 132.46, 133.83, 138.71, 146.44, 146.98, 149.79, 166.28; MS (m/z): 400 (M^+, 27.25), 77 (100.00). Anal. Calcd. for $C_{22}H_{20}N_6S$ (400): C, 65.98; H, 5.03; N, 20.98. Found: C, 65.95; H, 5.00; N, 20.96.

3-(Neopentylthio)-5,7-diphenyl-7H-pyrazolo[4,3-e][1,2,4]triazolo[4,3-c]pyrimidine (10)

White solid; reaction time: 1 h yield 68% (0.28 g); m.p. 152-154 °C; IR (KBr, ν, cm^{-1}): 3072 (Ar-H), 2955 (Aliph-H).); ^{1}H-NMR (DMSO-*d6*, δ, ppm): 1.05 (s, 9H, --SCH_2-$C(CH_3)_3$), 3.41 (br. s., 2H, , --SC**H**$_2$-$C(CH_3)_3$), 7.44 – 8.44 (m, 10H, Ar-H), 8.79 (s, 1H, Ar-H, C3–H pyrazole); ^{13}C-NMR (DMSO, 100 MHz): 28.85, 32.16, 46.66, 102.83, 122.70, 127.81, 128.80, 129.18, 130.94, 131.71, 132.46, 133.51, 138.71, 146.44, 146.91, 149.14, 166.95; MS (m/z): 414 (M^+, 27.25), 77 (100.00). Anal. Calcd. for $C_{23}H_{20}N_6S$ (414): C, 66.64; H, 5.35; N, 20.27. Found: C, 66.60; H, 5.33; N, 20.31.

3-(Cyclopentylthio)-5,7-diphenyl-7H-pyrazolo[4,3-e][1,2,4]triazolo[4,3-c]pyrimidine (11)

White solid; reaction time: 1.5 h yield 58% (0.24 g); m.p. 135-137 °C; IR (KBr, ν, cm^{-1}): 3080 (Ar-H), 2950 (Aliph-H). ^{1}H-NMR (DMSO-*d6*, δ, ppm): 1.61 - 1.78 (m, 8H), 4.07 (br. s., 1H), 7.46 – 8.45 (m, 10H, Ar-H), 8.76 (s, 1H, Ar-H, C3–H pyrazole); ^{13}C-NMR (DMSO, 100 MHz): 25.55, 35.75, 42.26, 103.03, 122.80, 127.81, 128.80, 129.18, 130.94, 131.71, 132.46, 133.58, 138.71, 146.48, 146.91, 149.18, 166.98; MS (m/z): 412 (M^+, 8.20), 288(100.00). Anal. Calcd. for $C_{23}H_{20}N_6S$ (412) C, 66.97; H, 4.89; N, 20.37. Found: C, 67.94; H, 4.92; N, 20.41.

3-((Cyclobutylmethyl)thio)-5,7-diphenyl-7H-pyrazolo[4,3-e][1,2,4]triazolo[4,3-c]pyrimidine (12)

White solid; reaction time: 1 h yield 70% (0.29 g); m.p. 139 - 141°C; IR (KBr, ν, cm^{-1}): 3075 (Ar-H), 2954 (Aliph-H). ^{1}H-NMR (DMSO-*d6*, δ, ppm): 1.77 - 1.88 (m, 4H), 2.06 - 2.15 (m, 2H), 2.76 (quin, J = 7.64 Hz, 1H), 3.48 (d, 2H, overlapped with H_2O), 7.45 – 8.45 (m, 10H, Ar-H), 8.79 (s, 1H, Ar-H, C3–H pyrazole); ^{13}C-NMR (DMSO, 100 MHz): 18.80, 27.53, 35.18, 47.25, 103.61, 122.60, 127.86, 128.60, 129.55, 130.94, 131.71, 132.46, 133.58, 138.71, 146.48, 146.91, 149.32, 166.32; MS (m/z): 412 (M^+, 3.90), 77 (100.00). Anal. Calcd. for $C_{23}H_{20}N_6S$ (412) C, 66.97; H, 4.89; N, 20.37. Found: C, 67.95; H, 4.92; N, 20.35.

Biological Activities Screening
In vitro antiproliferative activities

The current synthesized compounds have been tested for their anti-cancer activities against three different cancer cell lines; hepatocellular carcinoma (HepG-2), human breast adenocarcinoma (MCF-7) and human colon cancer (HCT-116), through neutral red assay protocol (Borenfreund et al. 1985). The Cell lines were cultured on DMEM media (Lonza) supplemented with 200 mM of L-glutamine and 10% of fetal bovine serum (FBS); Gibco-BRL. The tested compounds were dissolved in a mixture of Dimethyl Sulfoxide and DMEM with ratio 4:100 (v/v), respectively. An initial dose of (1 mg/ml) was tested on all cell lines and subsequences by seven more dilutions using value of 50% as dilution factor from the starting dose. Cells were seeded with concentration of (6 × 104 cell/ml) for 24 hours in flat bottom 96 well plates at 5% CO_2 and 37°C until semi confluent cell layer was obtained then, treated with 100 µl of each of serially diluted compounds. After 48 hours, the anticancer activity of the compounds was measured quantitatively by ELISA microplate reader at wave length 540-nm using neutral red assay protocol. Doxorubicin was used as a positive control. The results of cytotoxicity were reported as IC_{50} values.

DNA intercalation assay (DNA/methyl green assay)

The synthesized compounds were tested for their DNA-binding affinities using the methyl green dye according to the reported procedure (Burres et al. 1992). A mixture of methyl green (20 mg) and Calf thymus DNA (10 mg) (Sigma– Aldrich) were suspended in 0.05 M Tris-HCl buffer (100 ml, pH 7.5) containing 7.5 ml of $MgSO_4$. This mixture was stirred continuously for 24 h at 37 °C. The tested compounds were dissolved in ethanol and pitted into the wells of a 96-well microtiter tray at a concentration of 10,100 and 1000 µM. The excess solvent was removed from each well under vacuum, with subsequent addition of 200µl of the DNA/methyl green solution. The test samples were incubated for 24 h in a dark at ambient temperature. Then, absorbance of each sample was determined at 642.5-645 nm. Readings were corrected for initial absorbance and normalized as the percentage of the untreated DNA/methyl green absorbance value. In this test, the methyl green dye reversibly binds DNA to form persistent colored complex of DNA/methyl green. This color still stable at neutral pH. When the DNA intercalators were added, the methyl green was displaced from DNA with addition of H_2O molecule to the dye resulting in formation of the colorless carbinol

leading to a decrease in spectrophotometric absorbance. ΔA value (the difference between DNA/methyl green complex and free cabinol) provides the simplest means for detecting the DNA-binding affinity and relative binding strength. IC_{50}'s were determined by linear regression of data plotted on a semi-log scale. The results of DNA-binding affinity are reported as IC_{50} values. Doxorubicin, as one of the most powerful DNA intercalators, was used as a positive control.

Topoisomerase II inhibitory activity

The most active compound was further examined as topo II inhibitors, according to the reported method (Singla et al. 2017) . In general, the reaction started upon incubation of a mixture consisted of human topo II (2 µl), substrate super coiled pHot1 DNA (0.25 µg), 50 µg/ml test compound (2 µl), and assay buffer (4 µl) in 37 ºC for 30 min. In order to terminate the reaction, 10% sodium dodecylsulphate (2 µl) and proteinase K (50 µg/ml) were added at 37 ºC for 15 min followed by incubation for 15 min at 37 ºC. Then, the DNA was run on 1% agarose gel in BioRad gel electrophoresis system for 1–2 h followed by staining with GelRedTM stain for 2 h and destained for 15 min with TAE buffer. The gel was imaged via BioRad's Gel DocTMEZ system. Both supercoiled and linear strands DNA were incorporated in the gel as markers for DNA-Topo II intercalators. The results were reported IC_{50} (50% inhibition concentration) values calculated from the concentration-inhibition response curve. Doxorubicin was also tested using the same procedure as a positive control. The IC_{50} values were calculated from the concentration–inhibition response curve.

Molecular docking

In the present work, we used AutoDock program (Morris et al. 1998). AutoDock is a suit of automated docking tools, which allows flexible ligand docking and freely available under the GNU general public license (Huey et al. 2007). AutoDock predicts how small molecules, such as substrates or drug candidates bind to a receptor of known 3D structure. AutoDock suit includes two main programs: the AutoGrid, which pre-calculates the grids describing the target protein and the AutoDock, which performs the docking of the ligand to the target protein.

The scoring function used is empirically derived, for empirical binding free energy force field that allows the prediction of binding free energies for docked ligands. AutoDock is based on the United Atom force-filed of AMBER, which uses only polar hydrogens, this helps to reduce the number of atoms that must be modelled explicitly during the docking, thus speeding up the calculations.

Conclusion

This research reported the design and synthesis a series of novel pyrazolotriazolopyramidine derivatives as potential antitumor agents. Thus, the new synthesized compounds were evaluated for in vitro against a panel of three cancer cell lines, HepG-2, MCF-7, and HCT-116. The anticancer activity results displayed that compounds **12**, and **11** exhibited the best significant anticancer activity among the newly synthesized compounds against all tested cell lines with IC_{50} values ranging from

12.41 to 22.18 µM compared with doxorubicin. Additionally, the most active compound was further evaluated for their topoisomerase II inhibitory activities and DNA intercalating affinities with IC_{50} values of 0.005 and 30 µM, respectively compared with reference ligand, doxorubicin, with IC_{50} values of 0.01 and 31 µM. Moreover, the docking studies were also performed to suggest possible explanation of the results obtained from topoisomerase II inhibitory activities. Finally, pyrazolotriazolopyramidine derivatives represent a talented starting point for further study as anticancer agents.

REFERENCES

Arthur, D. E. (2019). Molecular docking studies of some topoisomerase II inhibitors: Implications in designing of novel anticancer drugs. *Radiology of Infectious Diseases, 6*(2), 68-79.

Bailly, C. (2012). Contemporary challenges in the design of topoisomerase II inhibitors for cancer chemotherapy. *Chemical reviews, 112*(7), 3611-3640.

Borenfreund, E., & Puerner, J. A. (1985). Toxicity determined in vitro by morphological alterations and neutral red absorption. *Toxicology letters, 24*(2-3), 119-124.

Burres, N. S., Frigo, A., Rasmussen, R. R., & McAlpine, J. B. (1992). A colorimetric microassay for the detection of agents that interact with DNA. *Journal of natural products, 55*(11), 1582-1587.

Cheng, C., & Robins, R. K. (1956). Potential purine antagonists. VI. Synthesis of 1-alkyl-and 1-aryl-4-substituted pyrazolo [3, 4-d] pyrimidines1, 2. *The Journal of Organic Chemistry, 21*(11), 1240-1256.

Denny, W. A. (2004). Emerging DNA topoisomerase inhibitors as anticancer drugs. *Expert opinion on emerging drugs, 9*(1), 105-133.

Ding, R., He, Y., Xu, J., Liu, H., Wang, X., Feng, M., . . . Peng, C. (2012). Preparation and bioevaluation of 99m Tc nitrido radiopharmaceuticals with pyrazolo [1, 5-a] pyrimidine as tumor imaging agents. *Medicinal Chemistry Research, 21*(4), 523-530.

Espinosa, E., Zamora, P., Feliu, J., & Barón, M. G. (2003). Classification of anticancer drugs—a new system based on therapeutic targets. *Cancer treatment reviews, 29*(6), 515-523.

Gaber, A. A., Bayoumi, A. H., El-morsy, A. M., Sherbiny, F. F., Mehany, A. B., & Eissa, I. H. (2018). Design, synthesis and anticancer evaluation of 1H-pyrazolo [3, 4-d] pyrimidine derivatives as potent EGFRWT and EGFRT790M inhibitors and apoptosis inducers. *Bioorganic Chemistry, 80*, 375-395.

He, H.-Y., Zhao, J.-N., Jia, R., Zhao, Y.-L., Yang, S.-Y., Yu, L.-T., & Yang, L. (2011). Novel pyrazolo [3, 4-d] pyrimidine derivatives as potential antitumor agents: exploratory synthesis, preliminary structure-activity relationships, and in vitro biological evaluation. *Molecules, 16*(12), 10685-10694.

Huang, Z.-H., Zhuo, S.-T., Li, C.-Y., Xie, H.-T., Li, D., Tan, J.-H., . . . Huang, S.-L. (2013). Design, synthesis and biological evaluation of novel mansonone E derivatives prepared via CuAAC click chemistry as topoisomerase II inhibitors. *European journal of medicinal chemistry, 68*, 58-71.

Huang, H., Chen, Q., Ku, X., Meng, L., Lin, L., Wang, X., . . . Li, M. (2010). A series of α-heterocyclic carboxaldehyde thiosemicarbazones inhibit topoisomerase IIα catalytic activity. *Journal of medicinal chemistry, 53*(8), 3048-3064.

Huey, R., Morris, G. M., Olson, A. J., & Goodsell, D. S. (2007). A semiempirical free energy force field with charge-based desolvation. *Journal of computational chemistry, 28*(6), 1145-1152.

Hurley, L. H. (2002). DNA and its associated processes as targets for cancer therapy. *Nature Reviews Cancer, 2*(3), 188.

Ibrahim, M., Taghour, M., Metwaly, A., Belal, A., Mehany, A., Elhendawy, M., . . . Hafez, E. (2018). Design, synthesis, molecular modeling and anti-proliferative evaluation of novel quinoxaline derivatives as potential DNA intercalators and topoisomerase II inhibitors. *European journal of medicinal chemistry, 155*, 117-134.

Islam, M. S., Park, S., Song, C., Kadi, A. A., Kwon, Y., & Rahman, A. M. (2017). Fluorescein hydrazones: a series of novel non-intercalative topoisomerase IIα catalytic inhibitors induce G1 arrest and apoptosis in breast and colon cancer cells. *European journal of medicinal chemistry, 125*, 49-67.

Kaina, B. (2003). DNA damage-triggered apoptosis: critical role of DNA repair, double-strand breaks, cell proliferation and signaling. *Biochemical pharmacology, 66*(8), 1547-1554.

Laponogov, I., Veselkov, D. A., Crevel, I. M.-T., Pan, X.-S., Fisher, L. M., & Sanderson, M. R. (2013). Structure of an 'open'clamp type II topoisomerase-DNA complex provides a mechanism for DNA capture and transport. *Nucleic acids research, 41*(21), 9911-9923.

Lee, J. H., Wendorff, T. J., & Berger, J. M. (2017). Resveratrol: a novel type of topoisomerase II inhibitor. *Journal of Biological Chemistry, 292*(51), 21011-21022.

Liu, L. F. (1989). DNA topoisomerase poisons as antitumor drugs. *Annual review of biochemistry, 58*(1), 351-375.

Miyashita, A., Iijima, C., & Higashino, T. (1990). Studies on pyrazolo [3, 4-d] pyrimidine derivatives. XVIII, Facile preparation of 1H-pyrazolo [3, 4-d] pyrimidin-4 [5H]-ones. *Heterocycles, 31*(7), 1309-1314.

Miyashita, A., Suzuki, Y., Iwamoto, K.-i., & HIGASHINO, T. (1998). Catalytic action of azolium salts. IX. Synthesis of 6-aroyl-9H-purines and their analogues by nucleophilic aroylation catalyzed by imidazolium or benzimidazolium salt. *Chemical and pharmaceutical bulletin, 46*(3), 390-399.

Mlcochova, P., Caswell, S. J., Taylor, I. A., Towers, G. J., & Gupta, R. K. (2018). DNA damage induced by topoisomerase inhibitors activates SAMHD1 and blocks HIV-1 infection of macrophages. *The EMBO journal, 37*(1), 50-62.

Morris, G. M., Goodsell, D. S., Halliday, R. S., Huey, R., Hart, W. E., Belew, R. K., & Olson, A. J. (1998). Automated docking using a Lamarckian genetic algorithm and an empirical binding free energy function. *Journal of computational chemistry, 19*(14), 1639-1662.

Nitiss, J. L. (2009). Targeting DNA topoisomerase II in cancer chemotherapy. *Nature Reviews Cancer, 9*(5), 338.

Pogorelčnik, B., Brvar, M., Žegura, B., Filipič, M., Solmajer, T., & Perdih, A. (2015). Discovery of Mono-and Disubstituted 1H-Pyrazolo [3, 4] pyrimidines and 9H-Purines as Catalytic Inhibitors of Human DNA Topoisomerase IIα. *ChemMedChem, 10*(2), 345-359.

Pommier, Y., Leo, E., Zhang, H., & Marchand, C. (2010). DNA topoisomerases and their poisoning by anticancer and antibacterial drugs. *Chemistry & biology, 17*(5), 421-433.

Schenone, S., Radi, M., Musumeci, F., Brullo, C., & Botta, M. (2014). Biologically driven synthesis of pyrazolo [3, 4-*d*] pyrimidines as protein kinase inhibitors: an old scaffold as a new tool for medicinal chemistry and chemical biology studies. *Chemical reviews, 114*(14), 7189-7238.

Shenkenberg, T. D., & VON HOFF, D. D. (1986). Mitoxantrone: a new anticancer drug with significant clinical activity. *Annals of internal medicine, 105*(1), 67-81.

Singla, P., Luxami, V., Singh, R., Tandon, V., & Paul, K. (2017). Novel pyrazolo [3, 4-d] pyrimidine with 4-(1H-benzimidazol-2-yl)-phenylamine as broad spectrum anticancer agents: synthesis, cell based assay, topoisomerase inhibition, DNA intercalation and bovine serum albumin studies. *European journal of medicinal chemistry, 126*, 24-35.

Sung, W. J., Kim, D. H., Sohn, S. K., Kim, J. G., Baek, J. H., Jeon, S. B., . . . Lee, K. B. (2005). Phase II trial of amsacrine plus intermediate-dose Ara-C (IDAC)

with or without etoposide as salvage therapy for refractory or relapsed acute leukemia. *Japanese journal of clinical oncology, 35*(10), 612-616

Thun, M. J., DeLancey, J. O., Center, M. M., Jemal, A., & Ward, E. M. (2010). The global burden of cancer: priorities for prevention. *Carcinogenesis, 31*(1), 100-110.

Varrica, M. G., Zagni, C., Mineo, P. G., Floresta, G., Monciino, G., Pistarà, V., . . . Amata, E. (2018). DNA intercalators based on (1, 10-phenanthrolin-2-yl) isoxazolidin-5-yl core with better growth inhibition and selectivity than cisplatin upon head and neck squamous cells carcinoma. *European journal of medicinal chemistry, 143*, 583-590.

Wang, J. C. (2002). Cellular roles of DNA topoisomerases: a molecular perspective. *Nature reviews Molecular cell biology, 3*(6), 430.

Whittaker, S. R., Walton, M. I., Garrett, M. D., & Workman, P. (2004). The Cyclin-dependent kinase inhibitor CYC202 (R-roscovitine) inhibits retinoblastoma protein phosphorylation, causes loss of Cyclin D1, and activates the mitogen-activated protein kinase pathway. *Cancer research, 64*(1), 262-272.

Zhao, Y., Ge, C. W., Wu, Z. H., Wang, C. N., Fang, J. H., & Zhu, L. (2011). Synthesis and evaluation of aroylthiourea derivatives of 4-β-amino-4'-O-demethyl-4-desoxypodophyllotoxin as novel topoisomerase II inhibitors. *European journal of medicinal chemistry, 46*(3), 901-906.

تصميم و تحضير والارساء الجزيئى وتقييم النشاط المضاد للسرطان لبعض مشتقات البيرازولوتريازولوبيريميدين الجديدة كمتداخلات محتمله مع الحمض النووي ومثبطات لانزيم توبوايزوميراز اثنان

اشرف حسن بيومي و *فرج فاروق شربيني و اسلام بسيوني القعيد و احمد عادل جابر

قسم الكيمياء العضوية - كلية الصيدلة بنين - جامعة الأزهر- مدينه نصر -القاهرة – مصر

*البريد الالكتروني للباحث الرئيسي : **Dr-farag-sherbiny@azhar.edu.eg**

الملخص :

تم تصميم و تحضير سلسله من مشتقات البيرازولوتريازولوبيريميدين الهجين الجديدة فى انتاجيه مفيدة صناعيا من خلال بعض المركبات الوسيطه وتم إثبات الصيغ البنائية للمركبات باستعمال جهاز الآشعة دون الحمراء وجهاز الرنين النووي والمغناطيسي ومطياف الكتلة هذا بالإضافة إلى التحليل الدقيق لعناصر المركبات التى تبين نسبة الكربون والهيدروجين والنتروجين فى المركبات. وقد تم تقييم جميع المركبات الجديدة بيولوجيا فى المختبر لانشطتها السامه للخلايا السرطانيه فى بعض انواع السرطان كسرطان الثدي وسرطان الكبد وسرطان القولون وكذلك تم تقييم كفاءة هذه المركبات الجديدة كمتداخلات مع الحمض النووي وقد تم اختيار انشط هذه المشتقات لاختباره كمثبط لانزيم توبوايزوميراز اثنان .

وتم إجراء الإختبارات البيولوجية على المركبات الجديدة فوجد أن لها تأثير مضاد السرطان وذلك بالمقارنة بالمضاد للسرطان (دوكسوروبيسين) كمرجع.

وقد اظهرت نتائج تقييم السمبه لهذة المركبات على النحو التالي بالنسبه للنشاط المضاد للسرطان فقد كانت اقوى النتائج هي للمركبان ١٢ و١١ حيث اظهرا التاثير الابرز ضد جميع الخلايا السرطانيه المختبره بنتائج تتراوح بين ١٢.٤١الى ٢٢.١٨ ميكرومول بالمقارنه بقيم نتائج الدوكسوروبسين كعقار محكم التي تتراوح بين ٨.١٧ الى ٩.٢٨ ميكرومول. بينما اظهر المركب ١٠ قيما متوسطه تتراوح بين ٣٣.٧٩ الى ٣٥.٤١ ميكرومول بالمقارنه بدوكسوروبسين اما باقي المركبات فقد كانت نتائجها اقل قوه بالمقارنه بالمركبات الاخرى. بالنسبه لتداخل هذه العوامل مع الحمض النووي فقد جاء ١٢ في المرتبه الاولى حيث تداخل مع الحمض النووي بصوره اقوى من تداخل دوكسوروبسين بقيمة ٣٠.٨١ ميكرومول اما المركبات ٩ و ١٠و ١١ فقد جاءت نتائجها بين ٣٨.٦٢ الى ٥٣.٤٨ ميكرومول مما يجعلها في المرتبه الوسطى بالمقارنه بالمضاد للسرطان دوكسوروبسين بينما اتى في المرتبه الاخيره المركب ٨. وقد تم اختبار اقوى هذه المركبات وهو المركب ١٢من حيث نشاطا مثبطا لنشاط انزيم توبوايزوميراز اثنان حيث اعطى نتيجه قويه وهي ٠.٠٥٥ ميكرومول وذلك بالمقارنه بدوكسوروبسين. وتم اجراء دراسات النمذجه لفهم ارتباط المركبات وعرقله انزيم التوبويزوميراز اثنان وتفسير النتائج البيولوجيه.

الكليمات المفتاحية : مضاد للسرطان ، مشتقات البيرازولوتريازولوبيريميدين ، توبوايزوميراز اثنان ، متداخلات مع الحمض النووي ، الارساء الجزيئى